INCREASING THE PRODUCTIVITY OF THE CZOCHRALSKI PROCESS APPLYING MACHINE LEARNING

F. Mosel[1], L. Kulhavy[2], D. Baccar[2]
[1] PVA Crystal Growing Sytems GmbH, Im Westpark 10-12, 35435 Wettenberg, Germany
[2] Technische Hochschule Mittelhessen, Wilhelm-Leuschner-Strasse 13, 61169 Friedberg
e-mail: frank.mosel@pvatepla.com
phone: +49 64168690-125, fax: +49 64168690-822

ABSTRACT: Monocrystalline silicon for the production of solar cells has to be provided cost-effectively in large quantities. The Czochralski (Cz) technique is currently the only manufacturing method that can ensure the availability of high-quality material in sufficient quantities. Even if the crystal growth technology is highly developed, increasing productivity while reducing crystallization costs remains a major challenge. The outstanding advantage of Cz technology is the possibility of the visual control of the growing crystal. This means that disturbances during the crystal growth process that may result in a loss of monocrystallinity referred to as structure loss can be identified in an early stage and appropriate countermeasures can be initiated. Visual monitoring of the entire growth process has to be automated to such an extent that a failure is automatically detected and an alarm is triggered. A reliable visual assessment must still be given by an experienced operator for the further course of action. In this article, we report on an ongoing project in which we are testing different possibilities to ensure an effective automated monitoring of the Cz process. In a continuation of the project, we also want to apply methods of machine learning in order to find any meaningful correlations between process parameters and crystal growth disorders.
Keywords: Czochralski, crystal growth, structure loss, machine learning

1 INTRODUCTION

Rapidly advancing climate change has highlighted the need for rapid transformation in energy production. Fossil fuels as energy sources have a global impact on CO_2 emissions and has to be replaced by renewable energy sources. In addition to the expansion of wind energy, photovoltaic solar cell technology based on monocrystalline silicon is currently the most cost-effective energy supplier. However, China has become the leader in module production on the global market. In the area of ingot production and wafering, China owns practically a monopoly position. This situation similarly affects the engineering construction required for photovoltaics, particularly the cost-effective production of competitive crystal-growing systems based on the Czochralski-technology (Cz-puller).

The geopolitical situation has triggered resilience efforts across Europe to regain a certain degree of independence from the Chinese market, especially in the photovoltaics sector. In addition to innovative construction of crystallization systems, crystal growing technology has to be optimized also from the perspective of cost pressure and maximum productivity. Unproductive process times and downtimes of the crystal pulling systems have to be minimized. The main trigger for unproductive process times is the loss of structure, which means a phase transition from the monocrystalline to the polycrystalline state of the growing crystal. Polycrystalline crystal material can no longer be used for further processing and means a loss of yield that has to be kept as low as possible. If there is a loss of structure during the crystal growth, the following options are available: The growth process can be continued, the crystal can be removed or the crystal can be melted back and a new crystallization process can be started. In any case, timely detection of structural loss is absolutely necessary. Since it is practically no longer possible for an operator to visually observe the crystallization process on an industrial scale, an automatic warning message in the event of a structure loss is indispensable.

In addition to the detection of a loss of structure, its avoidance has the highest priority. In the Cz-process, with ever larger diameters and simultaneously increasing pulling speeds of the growing crystal, the thermo-mechanical stresses increase, which ultimately lead to an increasing probability of structure loss. The connection between the thermal stresses that occur in industrial Cz growth arrangements and the formation of dislocations has not been fully understood yet. The causes that initiate a loss of structure are diverse and still the subject of investigations. The distribution and level of the thermal stresses in the growing crystal, process parameters, the quality of the starting materials and consumables as well as process conditions that are difficult to quantify have to be taken into account. Hendawi's diagram provides an overview of some of the possible triggers for the occurrence of a structure loss.

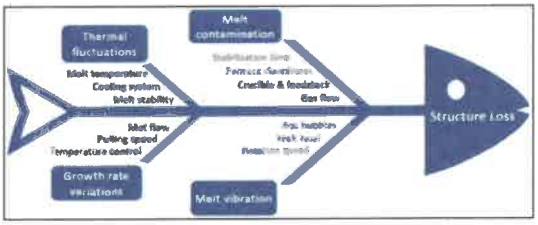

Figure 1: Fishbone diagram illustrating the main root causes of structure loss during the Cz growth of silicon [1]

2 APPROACH

In this paper we present an ongoing project in which a reliable method for automatic structure loss detection is being developed. The monocrystallinity of a growing crystal is accompanied by the formation of growth lines, which appear as vertical linear structures on the crystal surface in the growth direction. In the case of <100> crystal orientation, a monocrystal exhibits four growth lines. As long as the growing crystal shows continuous growth lines, it has a monocrystalline structure. The disappearance of these growth lines during the growth process is an indication that dislocations have formed that have multiplied due to the thermo-mechanical stresses in the growing crystal and ultimately triggered polycrystalline growth, i.e. a loss of structure. By means

10.4229/EUPVSEC2024/1BV.5.7
020027-001

of the process camera, which is used for diameter control, the presence of these growths lines, which are rotating with the crystal rotation rate, can be monitored. Two different possibilities for the detection of growth lines were taken into consideration. The growth line can be detected using a grayscale evaluation of the monochrome process image in the area of the bright meniscus region, which reflects the crystallization front of the growing crystal as shown in fig.2. Fig.3 shows the corresponding grey values along the red line sketched in Fig.2. This method of image evaluation is very complex because the position of the melt meniscus constantly changes due to diameter fluctuations and fluctuations of the melt level. Complicating matters are pendulum movements of the crystal and varying lighting conditions during the process. In addition, the growth lines may have different patterns depending on the temperature conditions at the phase boundary [2]. This type of image evaluation seems to be automatable only with great effort. We are therefore currently investigating various methods of convolutional neural networks (CNNs) to develop a reliable and robust method for the detection of the presence or absence of the growth lines.

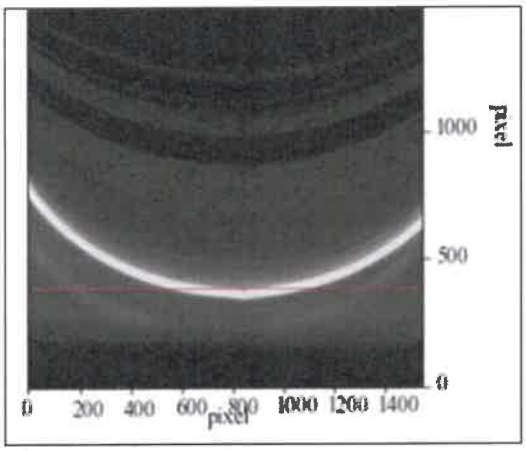

Figure 2: Detail of a process image showing the growth line entering the bright meniscus region and the red line of grey level evaluation.

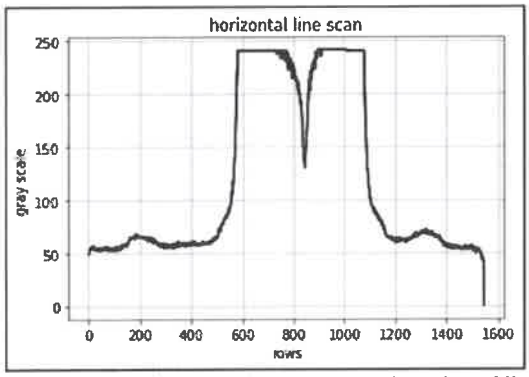

Figure 3: Distribution of the grey values along the red line in fig.2

3 EXPERIMENTAL

3.1 Crystal growth

The crystal growing process sequence can be divided into individual process steps (fig.4), which are already mostly automated. Nevertheless, observation of critical process phases, particularly the dipping phase and the subsequent start of the necking, are often still carried out manually by experienced operators.

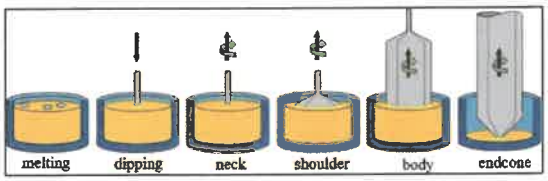

Figure 4: Process phases of a crystal growth run

The melting phase is followed by a certain period of time for the homogenization and stabilization of the melt volume. During the subsequent entire growth process from neck to endcone the diameter of the growing crystal is controlled by means of the process camera and monitored by visual observation. For our investigations, the images of the process camera were recorded from crystal growth processes executed in two different Cz-growers under completely different process conditions. In one of the two growers (SC24) 8-inch crystals were grown and in the other one (SC32) 12-inch crystals were grown under magnetic field conditions.

3.2 Data preparation

The difference in 8-inch and 12-inch crystal growth processes was taken into account in the data preparation as well as in the architecture of the convolutional neural networks. This means that in the first step the images were processed separately according to the two different Cz-growers. The process camera of both Cz-growers is an industrial monochrome camera with a resolution of 2064 x 1545 pixels. Since the CNNs (Convolutional Neural Networks) involve supervised learning, the images had to be classified into the two categories "mono" and structure loss "sl". The classification itself, i.e. deciding based on the appearance of the growth lines in the recorded process images whether there is a structure loss or not, proved to be very challenging and not always clear.

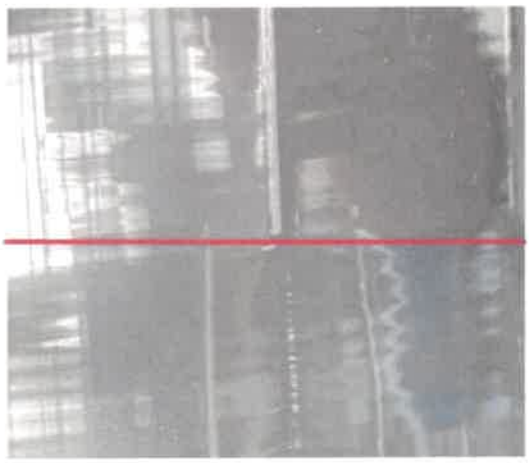

Figure 5: Abrupt end of a growth line, indicated by the red line

The growth lines often have an indifferent appearance. A sudden rupture of growth lines as shown in fig.5 is clear, but is only one possibility among many that indicate a loss

10.4229/EUPVSEC2024/1BV.5.7
020027-002

of structure. Fig.6 shows different characteristics of a growth line on the surface of a crystal. In the upper area up to the green line the growth line is undisturbed, in the middle area up to the red line the growth line shows an indifferent appearance, which suggests the presence of dislocations. In the lower part of the green line the crystal exhibits clearly a polycrystalline structure. Due to these uncertainties in the classification, the process images had to be reclassified or to be classified differently after the first training sessions, in order to remove uncertainties of the image selection. In the context of this report, only the body phase of the growing crystal was evaluated, since no structure losses occurred in the shoulder phase in our crystal growth experiments.

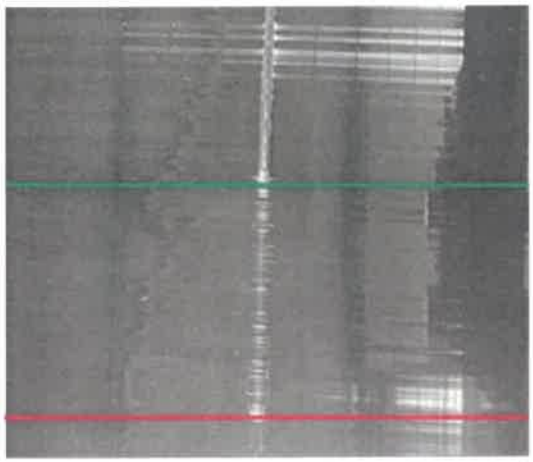

Figure 6: Different appearances of the growth line on the crystal surface

3.3 Convolutional Neural Network (CNN) Setup

Fig.7 shows the architecture of a CNN in a simplified representation. In several layers, the essential features of the classified images are extracted through several training sequences (Feature Extraction) and fed into a one-dimensional vector for classification. The result is given by the output vector ("mono" or "sl). The training runs are repeated until the error between input and output is minimal, for details see [3].

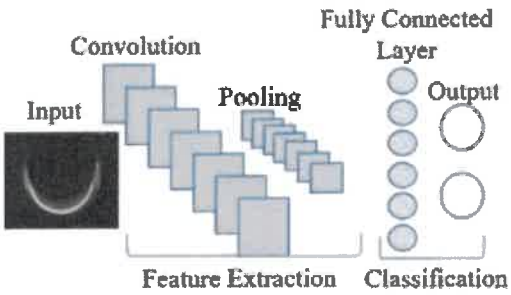

Figure 7: Architecture of a Convolutional Neural Network

For the project presented in this contribution, D. Baccar has developed an extremely efficient software tool that allows the user to create and use convolutional neural networks without writing any explicit program code [4]. The developer has the option of designing the networks from scratch or using the transfer learning strategy [5]. Various transfer networks are available in this software tool, which can be selected via a pull-down menu (Fig.8). Well-known basic networks are, for example, VGG16 and VGG19, which have a linear network architecture and the different ResNets, which use so-called residual blocks in their structures. The number at the end of the network name represents the number of convolutional layers used. Basic networks with a few layers are interesting for applications with short inference times. During transfer learning, the transfer networks are adapted to the specific data of the new classification task. This can be done by training the entire transfer network or just specific layers. This type of model creation saves time and resources. The software tool presented here is based on the Pytorch framework, the use of a GPU is recommended. All models in our project were trained on an Intel Core i9/2.6 GHz with GeForce RTX 4070 GPU, 32GB RAM.

3.4 Model training and evaluation of CNN

Various transfer networks with different hyperparameters were tested. Fig.8 and fig.9 show two screenshots of the software tool with the applied parameters for the example of ResNet 18. The selected hyperparameters proved to be suitable for several different transfer networks. The corresponding performance metrices of a training run of 6695 images are given in fig.10 and fig.12.

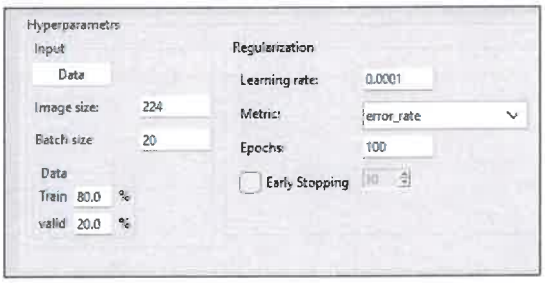

Figure 8: Screenshot of the user interface

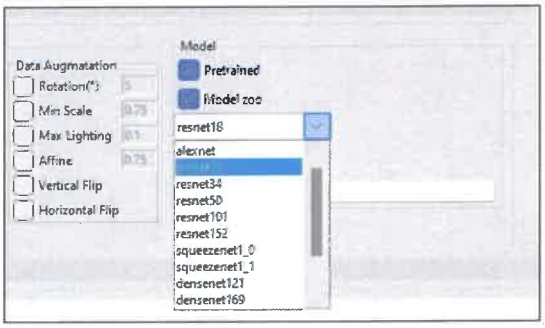

Figure 9: Screenshot of the user interface showing a small selection of available transfer nets

During training, the train loss and validation loss are recorded versus the epochs to show the progress of training performance (fig.11). The best model is continuously updated and saved. The corresponding data with a time stamp are recorded. All relevant training data as well as the model are stored and can be reloaded for optimization purposes. The training ends after the last epoch is completed and shows the confusion matrix of the validation data (fig.12). The rows of the matrix show the labeled values, the columns the calculated values. Using the confusion matrix, the key figures "accuracy" and "precision" of a classification can be deduced.

10.4229/EUPVSEC2024/1BV.5.7
020027-003

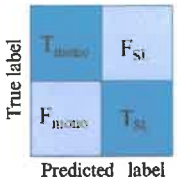

$$accuracy = \frac{T_{mono}+T_{SL}}{T_{mono}+T_{SL}+F_{mono}+F_{SL}}$$

$$precision = \frac{T_{mono}}{T_{mono}+F_{mono}}$$

Figure 10: Confusion matrix and key figures of evaluation (T: true values, F: false values)

In our models, mainly based on transfer nets, the validation curves consistently show better values than the training curves, which may be due to the simplicity of the classification. A performance of 100% of the validation could be achieved for all applied transfer models.

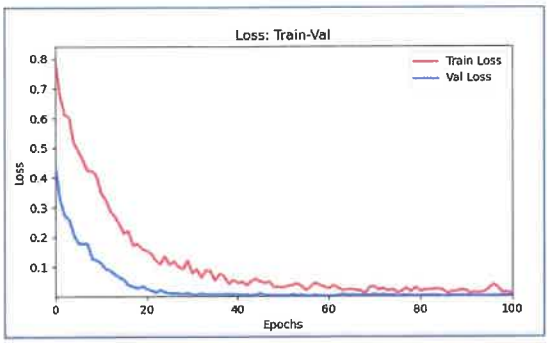

Figure 11: Train-loss and validation-loss versus training runs (epochs)

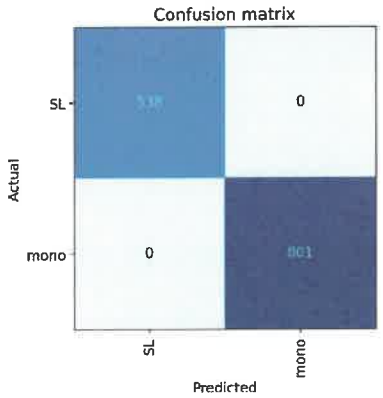

Figure 12: Confusion matrix of a completed training

However, the inference of our CNN-models showed a completely different picture for all models. 1000 test images, solely used for the inference, consisted of equal parts of mono-classified and SL-classified images (500 images each part). In both the training data and the test data, the absence of a growth line in the bright meniscus region was classified as a structure loss ("sl"). During monocrystalline growth, the slightly darker growth line extends into the bright meniscus ring-shaped region, as shown in fig.13 (red circle), which is no longer observed in the event of a structure loss, as shown in fig14 (yellow circle).

Figure 13: Process image classified "mono" with growth line visible in the meniscus region

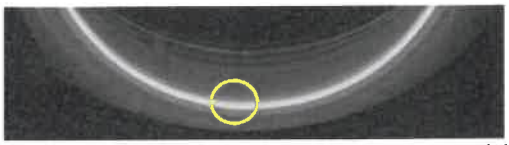

Figure 14: Process image classified "sl" with growth line outside the meniscus region

Figure 15: Process image classified "sl" with absence of growth line

Further stricter image classification, i.e. without the visibility of a growth line (fig.15), revealed that all images were classified as mono as soon as even a small fraction of a growth line was visible in the test images. Only images in which a growth line, i.e. a vertical structure, was not visible, provided the required inference result "sl". Fig.16 shows feature maps of ResNet18 without vertical structure (left), with partly vertical (middle) and completely vertical structure (right).

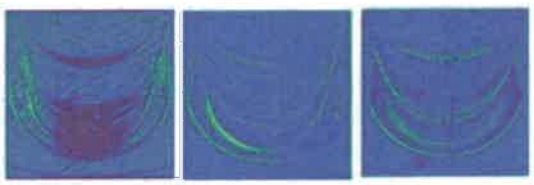

Figure 16: Feature maps of ResNet 18.

Corresponding histograms of the inference results are shown in fig.17 and fig.18.

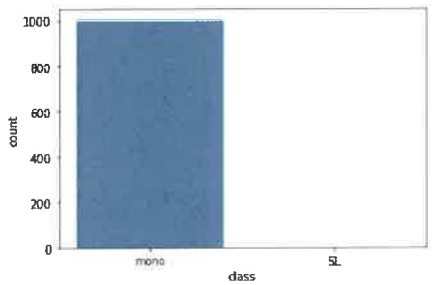

Figure 17: Histogram of inference executed on test-images, before strict classification (with partly vertical structure in the test images)

10.4229/EUPVSEC2024/1BV.5.7
020027-004

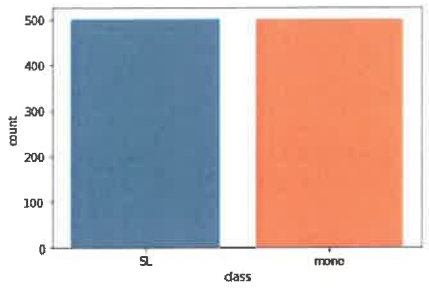

Figure 18: Histogram of inference executed on test-images after strict classification (without vertical structure in the test images)

The test results show that an early detection of a structure loss by means of a standard CNN is difficult to realize. Therefore, a region-based convolutional network (R-CNN) could be used in the area of the bright meniscus ring. Based on Zhang et al., a Faster R-CNN architecture was set up and trained [6].

3.5 Region based Convolutional Neural Network (Faster R-CNN) Setup

For the detection of the growth lines near the crystallization front, the use of a Faster R-CNN architecture is recommended as a model with a fast inference time for real-time detection. The principle of the architecture is shown in fig.19.

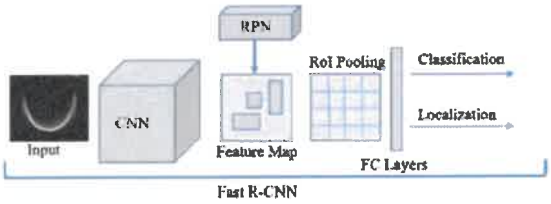

Figure 19: Architecture of the Faster R-CNN network

The Faster R-CNN architecture consists of two networks, Fast R-CNN and RPN (Region Proposal Network). The Fast R-CNN module creates a feature map from the input image using a pretrained CNN model. The RPN module is a fast network that recognizes objects and their location (bounding box) in the feature map of the CNN. The kind of the objects are unknown. These object proposals are fed into the Fast R-CNN network as RoIs (Region of Interest). A RoI pooling layer performs a max-pooling operation on the RoIs of nonuniform shape to obtain small fixed-size feature maps. The output contains two fully connected layers, a classification layer for the class probability ("mono" and "sl") and a bounding box regression for localization of the object, which is unimportant for our purposes. During training, a combined error of classification and localization is calculated and compared with the classified input until the error is minimal. The big advantage of the Faster R-CNN architecture for our application is the ability to limit an area in the image for training the network. In order to detect structural loss early, we limited the object search area by setting the ground truth boxes in a small area over the crystallization front as sketched (red rectangles) in fig.20 and fig.21.

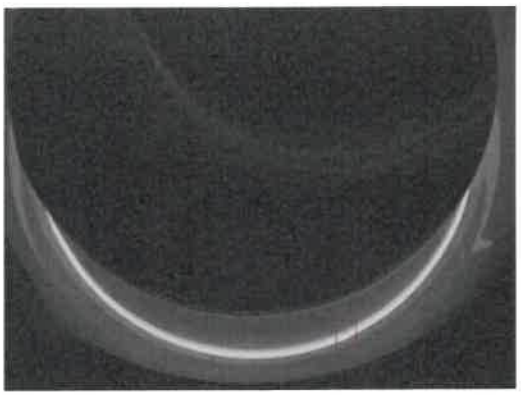

Figure 20: Bounding box for detection of the growth line in process image

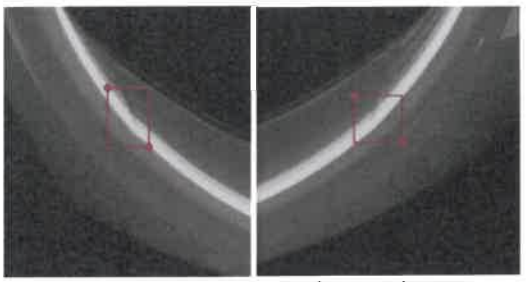

Figure 21: Detail enlargements of process images

3.6 Model training and evaluation of Faster R-CNN

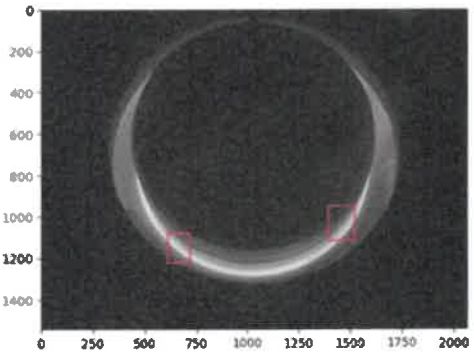

Figure 22: bounding box localization with growth line on a test image

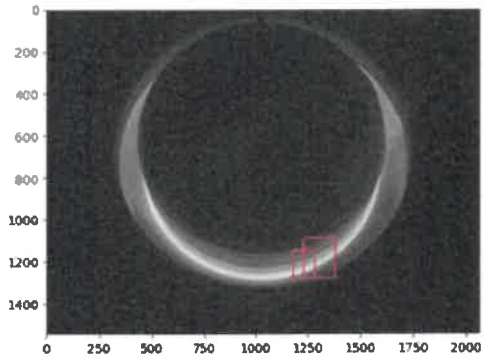

Figure 23: Overlapping bounding boxes on a growth line on a test image

10.4229/EUPVSEC2024/1BV.5.7
020027-005

The classified process images with the original size of 2064 x 1545 pixels together with the corresponding coordinates of the ground truth boxes are loaded as input into the transfer network ResNet50. The hyperparameters used are a batch size of 4 images and 100 epochs with a learning rate of 0.0001. The data split was 90% for training and 10% for inference. Also in this Faster R-CNN architecture, the training loop is run through until the deviation from the output combined from classification and localization to the input is minimal. Fig.22 and fig.23 show two examples. In both cases, the growth lines were located in the light meniscus area and were also correctly classified as mono. The amount of images, especially in the case of structure loss, was not sufficient to present a meaningful model. However, the results so far are promising.

3.7 Analysis of process parameters from the perspective of structure loss

The connection between dislocation formation and thermal stresses in the growing crystal is established by a critical shear stress CRSS-model (Critical Resolved Shear Stress) [7]. The temperature dependence of the critical shear stresses in the silicon glide system is shown in fig.24 for various authors [8].

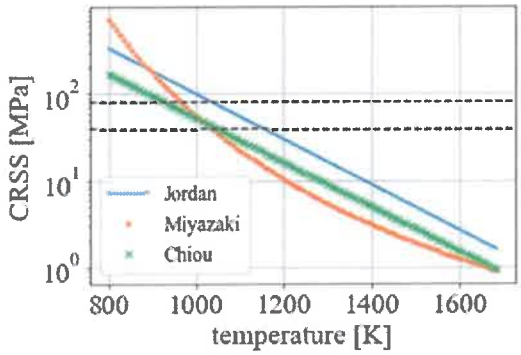

Figure 24: CRSS in the glide system for silicon [8]

The published values are in the range of 1-2 MPa at the solidification temperature. The thermal stresses that occur in industrial Cz-crystal growth configurations are in the range of 40 and 80 MPa (dashed lines) [9]. This means that monocrystalline silicon crystals can be grown successfully in the region of this supercritical thermal stress field (fig. 24). This discrepancy can be explained by a qualitative model of Muiznieks et al [10]. It is assumed that the crystal is in a metastable state concerning the critical thermal stress during growth and requires some additional energy contribution to leave this metastable state. It is assumed that only the local level of thermal stress is crucial for dislocation formation and not the mean thermal stress distribution in the crystal volume. This additional energy contribution can be delivered by temperature fluctuations, local melt-back effects or other growth disturbances in the area of solidification. This additional energy contribution decreases as the level of stress in the crystal increases. Since the root-causes that trigger a structure loss can be diverse and in some cases have not yet been clarified, they cannot be classified. Therefore, an unsupervised learning method has to be used in machine learning in order to find correlations to process parameters. AutoEncoder seems to be a suitable neural network to identify process anomalies. AutoEncoders are trained exclusively with process data representing perfect process conditions. The functionality is outlined in fig.25.

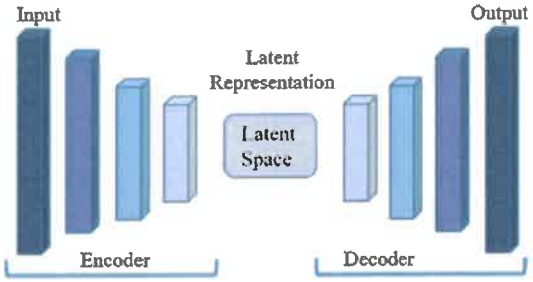

Figure 25: Diagram of AutoEncoder network

The input data are compressed into the latent space in the neural network of the AutoEncoder. All information from the undisturbed process are available in reduced form in the latent space. Decoding the latent space trains the network to reconstruct the input data as best as possible. The aim of this procedure is to learn undisturbed process data. During inference, i.e. applying the trained model to undisturbed process data, the AutoEncoder will reconstruct the process data as best as possible. If the process data are disturbed or show anomalies, the reconstruction will reveal anomalies.

3.8 Model training and evaluation of AutoEncoder

To analyse the process variables that can trigger a loss of structure, among other things, we had access to the process data of 103 crystal growth runs, all of which took place in a Cz puller under process conditions that were as similar or at least comparable as possible. A total of 150 process variables were recorded every 5 seconds. The structure losses were recorded in time by operators. Of the 103 processes, 71 processes were finished completely monocrystalline, 5 processes were completed with a loss of structure, which resulted in a complete loss of the material, in the other processes the crystals with a structure loss were still usable to a large extent. Of the 71 processes that were completed as mono crystals, 32 processes were carried out without any failure, i.e. remelting after structure loss. These process data are therefore predestined for training processes for perfect process conditions. In the first step of our model building, the input data were converted into matrices, with 93000 time steps and 12 process parameters (out of 150). The output data had the same format. The batch size was one process each, the training duration was 100 epochs with a learning rate of 0.0001. The network which was programmed from scratch consisted of 5 hidden layers, two for the contracting and two for the expanding path, one layer for the latent space. Fig.26 and fig.27 show two example results of an inference shown as a rectangular matrix. The time steps over the reconstruction errors of 12 process parameters are shown in a heatmap representation. Fig27. shows anomalities in the process parameters 3 and 4 that lie in the same range of time. If a loss of structure is recorded at a slightly later point in time, this could be an indication of a correlation of a structure loss and process parameters.

10.4229/EUPVSEC2024/1BV.5.7
020027-006

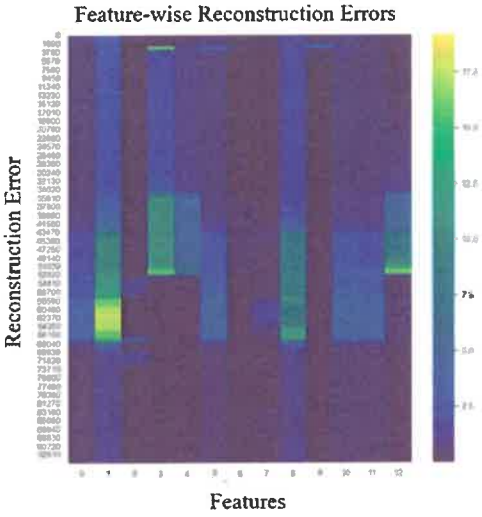

Figure 26: Heat map of the reconstruction error (time scale) versus 12 process parameters (out of 150)

The examples shown here are intended to demonstrate a general possibility of examining correlations in process parameters through the use of machine learning.

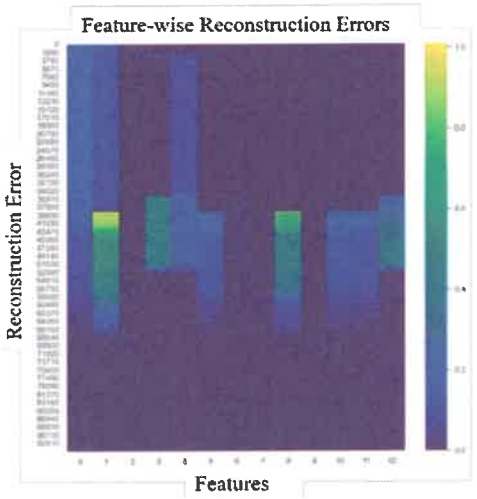

Figure 27: Heat map of the reconstruction error (time scale) versus 12 process parameters (out of 150)

At this point, it should be noted that we are just at the very beginning of analyzing the process parameters by means of machine learning.

4 SUMMARY

In this report, we present the status of our ongoing project work on structure loss of silicon monocrystals grown by the Cz-technology. The project is split into two parts. In one part, an automatable method is to be developed, that bases on machine learning methods, detects a structure loss or other anomalies of the growing crystal at an early stage. The results achieved so far with a region-based convolutional neural network are very promising. However, the model creation is not yet been complete, which is also due to the fact that only a limited number of suitable process images are available. Alternative network architectures need to be investigated.

In the second part of our project, various machine learning methods will also be examined in order to find correlations to the process conditions in the recorded process data. The root causes that led to the correlations found should be clarified in order to contribute to process optimization.

5 ACKNOWLEDGEMENTS

This work was supported by the German Federal Ministry for Economy Affairs and Climate Action under contract number 03EE1126B

6 REFERENCES

[1] R. Hendawi, Marisa Di Sabatino, Journal of Crystal Growth **629** (2024), 127564
[2] L. Stockmeier et al., Journal of Crystal Growth **512** (2019), 26-31
[3] Ian Goodfellow, Yoshua Bengio, Aaron Courville, Deep Learning, Adaptive Computation and Machine Learning Series, Cambridge, Mass.: MIT press Ltd, (2017)
[4] D. Baccar, Technische Hochschule Mittelhessen, dorra.baccar@m.thm.de
[5] Karl Weiss et al.,Journal of Big Data 3.1 (2016)
[6] Jun Zhang et al., Appl. Sci. 2020, 10, 7799; doi:10.3390/app10217799
[7] A. S. Jordan, R. Caruso, A. R. Von Neida, Bell. Syst. Tech. Journ. **59** (1980) 593
[8] G. Raming, Fortschritt-Berichte VDI Reihe 9 Nr. 330, VDI-Verlag Düsseldorf, 2001, S.133
[9] W. von Ammon, E. Dornberger, P.O. Hansson, Journal of Crystal Growth **198/199** (1999) 390
[10] A. Muiznieks et al., Journal of Crystal Growth **230** (2001), 305-313